Appl. Phys. B 61, 27–32 (1995)

Applied Physics B Lasers and Optics



# Three-valence charge-transport model for explanation of the photorefractive effect

**K. Buse, E. Krätzig**

Universität Osnabrück, Fachbereich Physik, D-49 069 Osnabrück, Germany
(Fax: +49-541/969-2670, E-mail: KBUSE@physik.uni-osnabrueck.de)

Received: 30 November 1994 / Accepted: 24 January 1995

**Abstract.** A new charge-transport model assuming one center in three different valence states is discussed for explanation of the photorefractive effect. Quantitative description of experimental results in $KNbO_3$:Fe by the model is demonstrated. Many similarities with the so-called "two-center" model are found although the microscopic explanation of the light-induced charge transport is rather different.

**PACS:** 61.70; 72.40; 78.20

Photorefractive crystals are promising materials for many applications, e.g., self-pumped phase conjugation, image processing, volume holographic storage or signal amplification [1]. The ferroelectric perovskites $KNbO_3$ and $BaTiO_3$ are of special interest because of large electrooptic coefficients and small response times. Tailoring of these crystals requires detailed knowledge of the light-induced charge transport and identification of the centers involved in the photorefractive process.

The so-called "one-center model" assumes that one center occurs in two different valence states, e.g. iron as $Fe^{2+}$ and $Fe^{3+}$ in $LiNbO_3$ crystals [2]. Then $Fe^{2+}$ ions act as filled and $Fe^{3+}$ ions as empty traps. If no space charge limiting effects are involved, this model predicts a photoconductivity increasing linearly with light intensity and an intensity independent absorption. Although the model describes the charge transport in $LiNbO_3$:Fe [2] at usual cw laser intensities ($< 100\ kWm^{-2}$), it fails to explain of the photorefractive effect in $KNbO_3$ and $BaTiO_3$. These materials show a nonlinear photoconductivity [3, 4, 5, 6] and light-induced absorption changes [7, 8, 9]. Similar effects are observed in $LiNbO_3$ at very high light intensities ($> 1\ MWm^{-2}$), too [10].

In 1988 Brost et al. [9] developed the "two-center charge-transport model"; two different centers are assumed, each of them occuring in two different valence states. The first center is deep and the second more shallow with respect to the band edge. For hole conductivity, the following processes take place: In the dark the shallow impurities are completely filled by thermally excited valence band electrons. Illumination excites electrons from the valence band into the deep center. With increasing intensity, the concentration of holes in the valence band certainly increases, but an appreciable amount is annihilated by electrons from shallow impurities. Thus a redistribution of electrons from the shallow into the deep center happens. This causes absorption changes if the cross sections of deep and shallow centers are different [9]. Holtmann [11] discovered that the model describes the nonlinear photoconductivity, too. Other authors [12, 13] explained this effect in the same manner.

The development of the two-center model was an important progress. Many further experimental results could be explained: Temperature dependence of photoconductivity $\sigma_{ph}$ and of light-induced absorption $\alpha_{li}$ [7, 14], a linear relation between $\sigma_{ph}^{-1}$ and $\alpha_{li}^{-1}$ [14], increase and decay of $\alpha_{li}$ [7], a linear relation between $\sigma_{ph}$ and light intensity $I$ at very large intensities [15], light-induced absorption generated by light pulses [16, 17], sensitization of the crystals for infrared recording by green illumination [18], dark build-up of holograms [19, 20, 21] or a photovoltaic effect increasing nonlinearly with light intensity [22, 23]. For these reasons, the two-center model has been widely accepted within a relatively short time. The model has been applied to other materials which show a nonlinear photoconductivity or light-induced absorption changes, e.g., to nonferroelectric sillenites [20] or to $Sr_{1-x}Ba_xNb_2O_6$ (SBN) [24, 25, 26]. Light–induced absorption measurements provide some hints that different shallow centers are present [17, 27] and consequently the most general case, a "n-center model", has been investigated [28].

But to our opinion there exists a further possibility to explain the experimental results described above. In this contribution we present a new charge-transport model which we call "three-valence model". One impurity center is assumed occuring in three different valence states. We derive predictions for photoconductivity and light-induced absorption changes, apply the results to experimental findings for $KNbO_3$:Fe and finally compare the consequences of the three-valence and the n-center model.

## 1 Three–valence model

The three-valence model assumes one center X occuring in three different valence states as illustrated by the band diagram in Figure 1. The valence states are denoted by 0, + and 2+. The arrows indicate the considered excitation and recombination processes of electrons. At low light intensities only $X^0$ and $X^+$ are present because thermally excited valence-band electrons fill $X^{2+}$. Illumination excites electrons from the valence band into $X^+$ and generates holes which are annihilated by electrons from $X^0$. For sufficiently high light intensities, the hole concentration becomes large enough that an appreciable number of electrons from $X^+$ can recombine with holes and generate $X^{2+}$ contributing to absorption. Thus light-induced absorption changes appear. Furthermore participation of $X^{2+}$ in the charge transport may provide a photoconductivity inreasing nonlinearly with light intensity. In the following we will treat the model more quantitatively.

Rate equations, charge conservation and constant trap density may be written as

$$\frac{dN^+}{dt} = +\underbrace{r^0 N^0 h}_{1} - \underbrace{(\beta^+ + q^+ S^+ I)N^+}_{2} - \underbrace{r^+ N^+ h}_{3} + \underbrace{(\beta^{2+} + q^{2+} S^{2+} I)N^{2+}}_{4} , \quad (1)$$

$$\frac{dN^{2+}}{dt} = +\underbrace{r^+ N^+ h}_{3} - \underbrace{(\beta^{2+} + q^{2+} S^{2+} I)N^{2+}}_{4} , \quad (2)$$

$$N_C = 2N^{2+} + N^+ + h , \quad (3)$$

$$N = N^0 + N^+ + N^{2+} . \quad (4)$$

Here $N^0$, $N^+$ and $N^{2+}$ are the concentrations of $X^0$, $X^+$ and $X^{2+}$, $N$ is the whole impurity concentration, $h$ is the concentration of holes in the valence band, $\beta^+$ and $\beta^{2+}$ are the thermal generation rates, $q^+$ and $q^{2+}$ are the quantum efficiencies for hole generation upon absorption of a photon, $S^+$ and $S^{2+}$ are the photon absorption cross sections, $I$ is the light intensity (in photons per $m^2$ and s), $r^0$ and $r^+$ are the recombination coefficients and $N_C$ is a constant concentration; an appropriate $N_C$ maintains overall charge neutrality. The numbers below the different terms in (1) and (2) correspond to the numbers of the arrows in the band diagram (Figure 1). We would like to emphasize that the three-valence model described by (1)–(4) is not a special case of the two-center model [9]; it is not possible to derive (1)–(4) by introducing a relation between the concentrations of deep and shallow traps.

### *1.1 Steady-state photoconductivity*

The hole concentration $h$ determines the photoconductivity $\sigma_{ph}$ by

$$\sigma_{ph} = e\,\mu\,h , \quad (5)$$

where $e$ is the elementary charge and $\mu$ the charge carrier mobility. In the steady-state situation ($dN^+/dt = 0$, $dN^{2+}/dt = 0$) and with a hole concentration $h$ small compared to $N^+$, the equations (1)–(4) yield

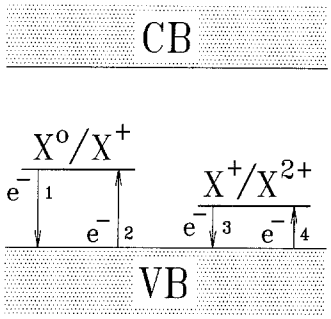


**Fig. 1.** Band diagram of the three-valence charge-transport model (*CB:* conduction band, *VB:* valence band). *Arrows* indicate excitation and recombination of electrons $e^-$ at $X^0$, $X^+$ and $X^{2+}$. The numbers relate to the different terms in the rate equations (1) and (2)

$$h = -\frac{\kappa^{2+}}{2r^+}\frac{N - N_C}{2N - N_C} + \left[\left(\frac{\kappa^{2+}}{2r^+}\frac{N - N_C}{2N - N_C}\right)^2 + \frac{\kappa^+\kappa^{2+}}{r^0 r^+}\frac{N_C}{2N - N_C}\right]^{1/2} , \quad (6)$$

where the symbols $\kappa^+ = \beta^+ + q^+ S^+ I$ and $\kappa^{2+} = \beta^{2+} + q^{2+} S^{2+} I$ are introduced for the generation terms. For small light intensities ($q^{2+} S^{2+} I \ll \beta^{2+}$ but $q^+ S^+ I \gg \beta^+$) the equations (5) and (6) yield a linear relationship $\sigma_{ph} \propto I$. For very large light intensities ($q^{2+} S^{2+} I \gg \beta^{2+}$ and $q^+ S^+ I \gg \beta^+$) a linear dependence $\sigma_{ph} \propto I$ is obtained, too. For $q^{2+} S^{2+} I \approx \beta^{2+}$, the photoconductivity increases nonlinearly with light intensity and can be described approximately by $\sigma_{ph} \propto I^x$ with $0.5 \leq x \leq 1$. These predictions are quite similar to those derived from the two-center model [11].

### *1.2 Steady-state light-induced absorption*

In the dark the absorption of the crystal is determined by $\alpha(I = 0) = N^+(0)S^+$; the concentration $N^{2+}(0)$ is much smaller than $N^+(0)$ because of the large thermal generation coefficient $\beta^{2+}$. Illumination generates a considerable concentration $N^{2+}(I)$ and because of charge conservation (equation (3)) we get $N^+(I) = N^+(0) - 2N^{2+}(I)$. Thus the absorption of the crystal illuminated with light of intensity $I$ is $\alpha(I) = (N^+(0) - 2N^{2+}(I))S^+ + N^{2+}(I)S^{2+}$. This yields for the light-induced absorption change

$$\alpha_{li} = \alpha(I) - \alpha(0) = N^{2+}(S^{2+} - 2S^+) . \quad (7)$$

Generation of one $X^{2+}$ center eliminates two $X^+$ centers: $2X^+ \rightarrow X^0 + X^{2+}$. This leads to the factor two in (7) and to a difference in comparison to the two-center model. The equations (2) and (7) yield for the light-induced absorption change in the steady-state situation

$$\alpha_{li} = (S^{2+} - 2S^+)N_C \times \left[2 + \beta^{2+}/(r^+ h) + q^{2+} S^{2+} I/(r^+ h)\right]^{-1} , \quad (8)$$

where $h$ can be calculated from (6).

### *1.3 Relation between photoconductivity and light-induced absorption*

From (5) and (8) we derive

$$\frac{1}{\alpha_{\mathrm{li}}} = \frac{1}{(S^{2+} - 2S^{+})N^{+}(0)} \times \left[2 + \left(\frac{\beta^{2+}}{r^{+}} + \frac{q^{2+}S^{2+}I}{r^{+}}\right)\frac{e\mu}{\sigma_{\mathrm{ph}}}\right] . \quad (9)$$

Thus for small light intensities ($q^{2+}S^{2+}I \ll \beta^{2+}$) a linear relation between $\alpha_{\mathrm{li}}^{-1}(I)$ and $\sigma_{\mathrm{ph}}^{-1}(I)$ is expected. The two-center model predicts such a relation, too [14]. However, interpretation of the parameters is different. Within the three-valence model we can determine the parameters $((S^{2+} - 2S^{+})N^{+}(0))^{-1}$ and $\beta^{2+}\mu/r^{+}$ with the help of (9).

### *1.4 Build–up and relaxation of light-induced absorption*

In order to evaluate simple formulas for the time evolution of $\alpha_{\mathrm{li}}$, the hole concentration $h$ is required. With the help of the adiabatic approximation (neglection of $\mathrm{d}h/\mathrm{d}t$ compared to $\mathrm{d}N^{2+}/\mathrm{d}t$ and $\mathrm{d}N^{+}/\mathrm{d}t$) the equations (1)–(4) yield

$$h = \frac{\kappa^{+}(N_{\mathrm{C}} - 2N^{2+}) + \kappa^{2+}N^{2+}}{r^{+}(N_{\mathrm{C}} - 2N^{2+}) + r^{0}(N + N^{2+} - N_{\mathrm{C}})} . \quad (10)$$

For sufficiently small light intensities ($q^{2+}S^{2+}I < \beta^{2+}$, $N^{2+}$ negligible in (10)), the hole concentration reaches a steady-state value before $N^{2+}$ changes considerably. We solve the rate equation (2) and obtain

$$\alpha_{\mathrm{li}}(t) = \alpha_{\mathrm{li},0}(1 - \exp(-\gamma_{\mathrm{li}}t)) , \quad (11)$$

$$\gamma_{\mathrm{li}} = (2r^{+}h + \beta^{2+} + q^{2+}S^{2+}I) , \quad (12)$$

where the steady-state value $\alpha_{\mathrm{li},0}$ is given by (8).

Considering (1)–(4) and (10), the decay of $\alpha_{\mathrm{li}}$ may be written in the form

$$\alpha_{\mathrm{li}}(t) = \alpha_{\mathrm{li}}(t = 0)\exp(-\beta^{*}t) , \quad (13)$$

$$\beta^{*} = \beta^{2+}(1 + \rho)^{-1} , \quad (14)$$

$$\rho = r^{+}(N_{\mathrm{C}} - 2N^{2+})/r^{0}(N + N^{2+} - N_{\mathrm{C}}) . \quad (15)$$

For $\rho \ll 1$ this decay is exponential with the decay rate $\beta^{*} = \beta^{2+}$. For $\rho > 1$ the decay rate $\beta^{*}$ depends on time through $N^{2+}(t)$ and its initial value defines a minimum for $\beta^{2+}$: $\beta^{2+} \leq \beta^{*}(t = 0)$.

The equations for the build-up and decay of light-induced absorption derived from the two-center model are again similar [7]. The reason is that the time evolution of $\alpha_{\mathrm{li}}$ is mainly determined by the rate equation (2) which has the same structure as that for the shallow center in the two-center model. But a significant difference occurs with the interpretation of the coefficient $\gamma_{\mathrm{li}}$. In the two-center model $\gamma_{\mathrm{li}}$ can be expressed very simply by parameters of the deep center [7]. Solving the rate equation (1) for $N^{+}$, however, yields a complicated time constant because four different processes may change $N^{+}$.

## 2 Application to $KNbO_3$:Fe

A very detailed investigation of photoconductivity and light-induced absorption changes for different light intensities and crystal temperatures was performed by Holtmann et al. for $KNbO_3$:Fe [7]. These authors demonstrated that the two-center model satisfactorily describes experimental results with a single parameter set. In this section we will check whether the three-valence model is able to explain the measurements of Holtmann et al., too. Experimental details can be found in [7].

**Table 1.** Model parameters used to explain the intensity dependence of photoconductivity and light-induced absorption for $KNbO_3$:Fe. The values of $\beta_1$ and $\beta_2$ are given for room temperature; $S^{+}$ and $S^{2+}$ are for $\lambda$ = 514 nm and light polarized perpendicular to the **c**–axis of the crystal

| Parameter | Value |
|---|---|
| $N$ | $1.5 \times 10^{24}$ m$^{-3}$ |
| $N_{\mathrm{C}}$ | $1.45 \times 10^{24}$ m$^{-3}$ |
| $q^{+}$ | 0.7 |
| $S^{+}$ | $1.1 \times 10^{-22}$ m$^{2}$ |
| $\beta^{+}$ | $1.8 \times 10^{-6}$ s$^{-1}$ |
| $r^{0}$ | $8.3 \times 10^{-15}$ m$^{3}$/s |
| $q^{2+}$ | 0.06 |
| $S^{2+}$ | $2.4 \times 10^{-22}$ m$^{2}$ |
| $\beta^{2+}$ | 0.15 s$^{-1}$ |
| $r^{+}$ | $1.5 \times 10^{-14}$ m$^{3}$/s |
| $\mu$ | $5 \times 10^{-5}$ m$^{2}$/Vs |

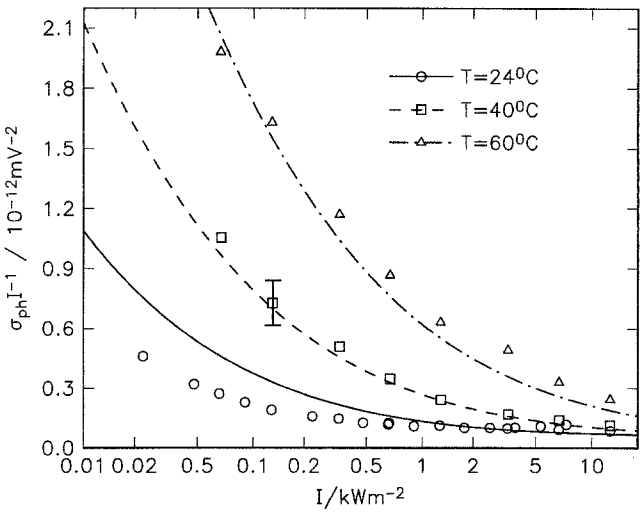


**Fig. 2.** Specific photoconductivity $\sigma_{\mathrm{ph}}/I$ versus light intensity $I$ for different crystal temperatures $T$. The symbols are measured results [7] and the curves are calculated from the three-valence model with the parameters of Table 1

The strategy is to leave only a few parameters free and to determine the other model parameters from the measured data. Then variation of the free coefficients is performed until optimal agreement between measured data and theoretical estimations is achieved. The varied parameters are $N_{\mathrm{C}}$ and $q^{+}$. For $\mu$ we use the value published by Holtmann et al. [7]. In the Appendix the determination of the complete parameter set is described. The obtained parameters are summarized in Table 1. It is important to note that the three-valence model has one parameter less than the two-center model. In the three-valence model we only have the impurity concentration $N$, while in the two-center model the concentrations of deep and shallow traps occur.

The Figures 2 and 3 show the specific photoconductivity $\sigma_{\mathrm{ph}}/I$ and the light-induced absorption change $\alpha_{\mathrm{li}}$ versus light intensity $I$ for different crystal temperatures. Fairly good agreement between measurements and calculations is obtained. The Figures 4 and 5 illustrate the time evolution of $\alpha_{\mathrm{li}}$ for switching on and off the pump light. The com-

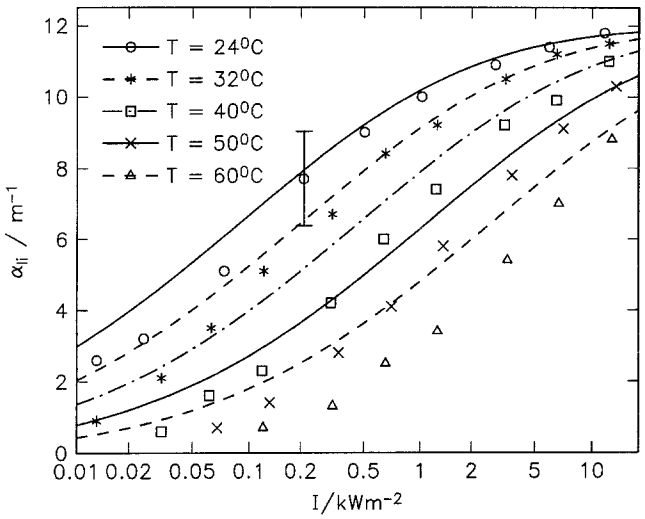


**Fig. 3.** Light–induced absorption coefficient $\alpha_{li}$ for $\lambda = 514$ nm as a function of light intensity $I$ for different crystal temperatures $T$. The symbols are measured results [7] and the curves are calculated from the three-valence model with the parameters of Table 1

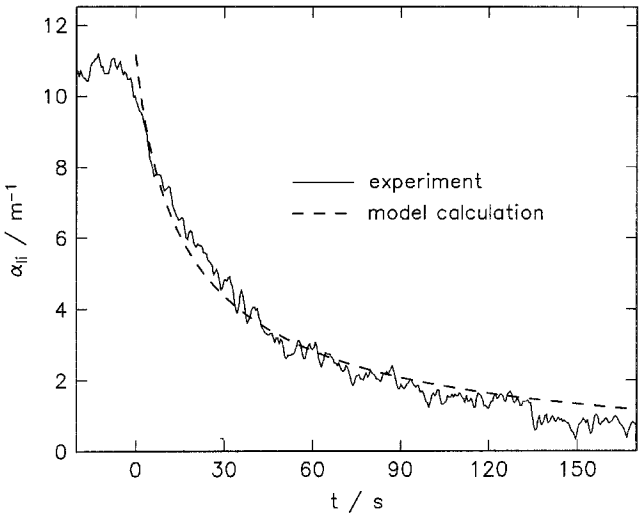


**Fig. 5.** Light–induced absorption coefficient $\alpha_{li}$ for $\lambda = 514$ nm versus time $t$. At $t = 0$ s the pump beam of intensity $I = 3$ kWm$^{-2}$ is switched off. The *solid curve* represents measured data [7] and the *dashed curve* is calculated from the three-valence model with the parameters of Table 1

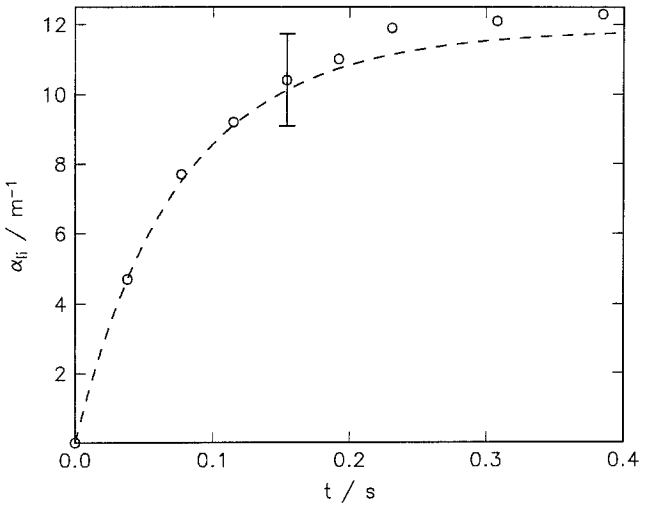


**Fig. 4.** Light–induced absorption coefficient $\alpha_{li}$ for $\lambda = 514$ nm versus time $t$. At $t = 0$ s a pump beam of intensity $I = 29$ kWm$^{-2}$ is switched on. The symbols represent measured data [7] and the curve is calculated from the three-valence model with the parameters of Table 1

puted curves are obtained by solving the rate equation (2) numerically with the help of the Runge–Kutta method using the adiabatic approximation (10). Good agreement between measured data and computations is again achieved.

Perhaps other parameter sets yield still smaller deviations. However, the calculations with the parameters of Table 1 demonstrate that the three-valence model enables a quite good description of the light-induced charge-transport properties in $KNbO_3$:Fe.

## 3 Discussion

In the introduction we have listed experimental findings which cannot be explained by a one-center model and consequently have led to the development of two-center models. But these findings can also be interpreted in terms of a three-valence model. Nonlinear increase of photoconductivity $\sigma_{ph}$ with light intensity $I$ (Section 1.1), light-induced absorption changes $\alpha_{li}$ (Section 1.2), temperature dependence of $\sigma_{ph}$ and $\alpha_{li}$ (Figures 2 and 3), the linear relation between $\sigma_{ph}^{-1}$ and $\alpha_{li}^{-1}$ (Section 1.3), increase and decay of $\alpha_{li}$ (Figures 4 and 5) and a relation $\sigma_{ph} \propto I$ for very large $I$ values (Section 1.1) directly follow from our analysis. Light–induced absorption generated by laser pulses can be understood if further valence states of the centers are assumed under intensive pulse illumination. Sensitization of the crystals for infrared recording by green illumination can be explained in the following way: Green light generates $X^{2+}$ impurities with energy levels close to the valence band allowing the excitation of valence band electrons into $X^{2+}$ with infrared light. Finally the nonlinear increase of the photovoltaic current with light intensity may result from contributions of both valence states, $X^{+}$ and $X^{2+}$, with different photovoltaic coefficients and the intensity dependence of the concentrations $N^{+}$ and $N^{2+}$.

In the present situation, the question if two-center model or three-valence model cannot be answered unambigously. Only the identification of centers and valence states involved could provide a key to the solution.

Light–induced charge-transport properties of transition-metal-doped $LiNbO_3$ crystals at usual cw laser intensities can be described by one-center models [2], but at high intensities additional effects (light-induced absorption, nonlinear photoconductivity) occur, pointing to the influence of further centers [10, 29]. Many investigations revealed the nature of the centers: $Nb^{5+}$ ions on $Li^{+}$ sites trap electrons and small polarons are formed under illumination [30]. If the number of polarons is reduced by decreasing the number of $Nb^{5+}$ ions on $Li^{+}$ sites, e.g. by doping with Mg or Zn, light-induced absorption is reduced [31], too, and photoconductivity scales linearly in $I$ [32]. For these reasons we think that the two-center model has to be applied for the description of photorefractive effects in $LiNbO_3$ at high light intensities.

But in the case of the ferroelectric perovskites $BaTiO_3$ and $KNbO_3$ we see some arguments in favour of the three-valence model. Numerous investigations were carried out with different samples, but always light-induced absorption and a nonlinear photoconductivity were observed. By doping, e.g. with iron [33], these effects are considerably increased. Thus the interpretation in terms of the two-center model yields a correlation between shallow and deep centers which is difficult to understand. The three-valence model, however, yields a correlation between different valence states which is obvious.

Three valence states of impurity centers in perovskites have indeed been found experimentally. Possenriede et al. investigated different $BaTiO_3$ samples by a combination of ESR and optical absorption measurements [34]. They showed that many different centers exist which may contribute to the photorefractive process. In all crystals they observed that $Fe^{3+}$ and $Fe^{4+}$ play a dominant role. Furthermore they found in all samples that illumination generates $Fe^{5+}$. Perhaps we can identify $X^{0,+,2+}$ with $Fe^{3+,4+,5+}$. An additional center which provides a three-valence system is chromium, occuring as $Cr^{3+,4+,5+}$ in $BaTiO_3$ [34].

Furthermore, Schunemann et al. showed [35] that iron doping increases the absorption of $BaTiO_3$ and that the absorption can be decreased by reducing treatments. These authors discovered that reduced samples have a much smaller and more linear photoconductivity ($\sigma_{ph} \propto I^x$ with $x$ close to 1) after reduction. This can be explained very well by the three-valence model. Iron doping increases the concentration $N^+(0)$ and thus enhances the crystal absorption. Reducing treatments decrease $N^+(0)$ and thus the absorption decreases. Furthermore, the photoconductivity decreases because the density $N^+$ of empty traps decreases and the density $N^0$ of filled traps increases. The smaller photoconductivity and the smaller concentration $N^+$ are responsible that only small concentrations $N^{2+}$ can be generated. Thus the influence of the third valence state on $\sigma_{ph}$ becomes weaker and the photoconductivity more linear in $I$. This interpretation leads to smaller light-induced absorption changes due to a smaller concentration $N^{2+}$ in reduced samples which has been confirmed by measurements of Temple and Warde [36] in $BaTiO_3$:Fe. – These are strong arguments that more than two valence states of impurities obviously have to be taken into account with the interpretation of photorefractive effects in perovskites.

*Acknowledgements.* We thank the Deutsche Forschungsgemeinschaft (SFB 225, C5) for financial support. Valuable discussions with H. Hesse, F. Jermann, R. A. Rupp and O. F. Schirmer are gratefully acknowledged.

## Appendix

Here we describe the procedure to determine all model parameters from the experimental results and from $N_C$, $q^+$ and $\mu$.

In the dark the concentrations $N^{2+}$ and $h$ are much smaller than $N^+$. Thus charge conservation (3) requires $N^+(0) = N_C$. The low intensity absorption is given by $\alpha(0) = N_C S^+ = 160\ m^{-1}$. This enables calculation of $S^+$. From (9) and from the measured linear relation between $\alpha_{li}^{-1}$ and $\sigma_{ph}^{-1}$ we deduce $(S^{2+} - 2S^+)N_C/2 = 14\ m^{-1}$. Together with the information $S^+N_C = 160\ m^{-1}$ we get $S^{2+}N_C = 348\ m^{-1}$ and use this for the determination of $S^{2+}$. The iron concentration in the crystal has been measured ($c_{Fe} = 1.5\times10^{24}\ m^{-3}$) and is assumed to be equal to $N$. From (5), (8) and (12) we derive $e\gamma_{li}\alpha_{li}\sigma_{ph}^{-1} = (S^{2+}-2S^+)N_C\, r^+/\mu$. Considering $(S^{2+} - 2S^+)N_C = 28\ m^{-1}$ the measured data yield $r^+/\mu = 3 \times 10^{-10}$ V. Together with $\mu$ we get the parameter $r^+$. For large intensities light-induced absorption saturates ($\alpha_{li} = \alpha_{li,sat}$) and the specific photoconductivity becomes constant ($(\sigma_{ph}/I) = (\sigma_{ph}/I)_{sat}$). From (5) and (8) we derive

$$q^{2+} = (\sigma_{ph}/I)_{sat}\, r^+ \left[(S^{2+} - 2S^+)N_C - 2\alpha_{li,sat}\right] \times(\alpha_{li,sat}S^{2+}e\mu)^{-1} . \quad (16)$$

The experiments give as results $\alpha_{li,sat} = 12\ m^{-1}$ and $(\sigma_{ph}/I)_{sat} = 6\times10^{-14}\ mV^{-2}$. These values, the parameters determined until now and (16) yield $q^{2+}$. The light-induced absorption changes should saturate for $I \geq I_{sat}$ with $I_{sat} = \beta^{2+}/(q^{2+}S^{2+})$. From the measurements we get $I_{sat} \approx 4\ kWm^{-2}$ at room temperature. Together with $q^{2+}$ and $S^{2+}$ this relation enables calculation of $\beta^{2+}$. For higher temperatures, appropriate $\beta^{2+}$ values are calculated from the Arrhenius law with an thermal activation energy of $E_A = 0.8$ eV. For large light intensities ($\kappa^+ \approx q^+S^+I$, $\kappa^{2+} \approx q^{2+}S^{2+}I$) the expression for the steady-state hole concentration (6) simplifies. Rearrangement of the equation yields with (5)

$$\frac{1}{r^0} = \left[\left(\frac{\sigma_{ph}}{I}\right)_{sat}^2 \frac{1}{(e\mu)^2} + \left(\frac{\sigma_{ph}}{I}\right)_{sat} \frac{1}{e\mu} \frac{q^{2+}S^{2+}}{r^+} \frac{N - N_C}{2N - N_C}\right] \times \frac{r^+}{q^+S^+q^{2+}S^{2+}} \frac{2N - N_C}{N_C} . \quad (17)$$

With the help of this equation we determine the coefficient $r^0$. Considering $\beta^{2+} \gg \beta^+$ we get from (5) and (6) for the steady-state dark conductivity the expression

$$\sigma_d = \sigma_{ph}(I = 0) = \frac{\beta^+}{r^0} e\mu \frac{N_C}{N - N_C} . \quad (18)$$

The experiment yields $\sigma_d = 5 \times 10^{-14}\ (\Omega m)^{-1}$. With the help of (18) we finally determine the parameter $\beta^+$.

## References

1. P. Günter, J.-P. Huignard (eds.): *Photorefractive Materials and Their Applications I, II*, Topics Appl. Phys., Vols. 61, 62 (Springer, Berlin, Heidelberg 1988)
2. E. Krätzig, O. F. Schirmer: In *Photorefractive Materials and Their Applications I*, ed. by P. Günter, J.-P. Huignard, Topics Appl. Phys., Vol. 61 (Springer, Berlin, Heidelberg 1988) pp. 131–166
3. P. Günter, F. Micheron: Ferroelectrics **18**, 27 (1978)
4. A. E. Krumins, P. Günter: Phys. Status Solidi (a) **55**, K185 (1979)
5. E. Krätzig, F. Welz, R. Orlowski, V. Doormann, M. Rosenkranz: Solid State Commun. **34**, 817 (1980)
6. S. Ducharme, J. Feinberg: J. Appl. Phys. **56**, 839 (1984)
7. L. Holtmann, K. Buse, G. Kuper, A. Groll, H. Hesse, E. Krätzig: Appl. Phys. A **53**, 81 (1991)
8. A. Motes, J. J. Kim: J. Opt. Soc. Am. B **4**, 1379 (1987)
9. G. A. Brost, R. A. Motes, J. R. Rotgé: J. Opt. Soc. Am. B **5**, 1879 (1988)
10. F. Jermann, E. Krätzig: Appl. Phys. A **55**, 114 (1992)

11. L. Holtmann: Phys. Status Solidi (a) **113**, K89 (1989)
12. D. Mahgerefteh, J. Feinberg: Phys. Rev. Lett. **64**, 2195 (1990)
13. G. A. Brost, R. A. Motes: Opt. Lett. **15**, 1194 (1990)
14. L. Holtmann, M. Unland, E. Krätzig, G. Godefroy: Appl. Phys. A **51**, 13 (1990)
15. K. Buse, E. Krätzig: Phys. Status Solidi **146**, K 37 (1994)
16. P. Ye, A. Blouin, C. Demers, M. D. Roberge, X. Wu: Opt. Lett. **16**, 980 (1991)
17. K. Buse, E. Krätzig: Opt. Mater. **1**, 165 (1992)
18. K. Buse, L. Holtmann, E. Krätzig: Opt. Commun. **85**, 183 (1991)
19. I. Biaggio, M. Zgonik, P. Günter: Opt. Commun. **77**, 312 (1990)
20. P. Tayebati, D. Mahgerefteh: J. Opt. Soc. Am. B **8**, 1053 (1991)
21. K. Buse, J. Frejlich, G. Kuper, E. Krätzig: Appl. Phys. A **57**, 437 (1993)
22. R. S. Cudney, R. M. Pierce, G. D. Bacher, D. Mahgerefteh, J. Feinberg: J. Opt. Soc. Am. B **9**, 1704 (1992)
23. K. Buse, H. Hesse, U. van Stevendaal, S. Loheide, D. Sabbert, E. Krätzig: Appl. Phys. A **59**, 563 (1994)
24. K. Buse, R. Pankrath, E. Krätzig: Opt. Lett. **19**, 260 (1994)
25. M. Simon, A. Gerwens, E. Krätzig: Phys. Status Solidi (a) **143**, K125 (1994)
26. S. Orlov, M. Segev, A. Yariv, R. Neurgaonkar: Opt. Lett. **19**, 1293 (1994)
27. G. A. Brost, R. A. Motes: Opt. Lett. **15**, 538 (1990)
28. R. S. Cudney, R. M. Pierce, G. D. Bacher, J. Feinberg: J. Opt. Soc. Am. B **8**, 1326 (1991)
29. F. Jermann, J. Otten: J. Opt. Soc. Am. B **10**, 2085 (1993)
30. O. F. Schirmer, O. Thiemann, M. Wöhlecke: J. Phys. Chem. Solids **52**, 185 (1991)
31. M. Simon, F. Jermann, E. Krätzig: Opt. Mater. **3**, 243 (1994)
32. M. Simon, F. Jermann, E. Krätzig: Appl. Phys. B (in press) (1995)
33. L. Holtmann, A. Groll, M. Unland, E. Krätzig, A. Maillard, G. Godefroy: Tech. Dig. Topical Meeting on Photorefractive Materials, Effects and Devices II 83 (1990)
34. E. Possenriede, P. Jacobs, H. Kröse, O. F. Schirmer: Appl. Phys. A **55**, 73 (1992)
35. P. G. Schunemann, D. A. Temple, R. S. Hathcock, H. L. Tuller, H. P. Jenssen, D. R. Gabbe, C. Warde: J. Opt. Soc. Am. B **5**, 1685 (1988)
36. D. A. Temple, C. Warde: Appl. Phys. Lett. **59**, 4 (1991)

This article was processed by the author using the LaTeX style file *pljour2* from Springer-Verlag.